NASA/TM–2013-218041

Active Noise Control of Radiated Noise From Jets

Michael J. Doty
Langley Research Center, Hampton, Virginia

Christopher R. Fuller
Virginia Polytechnic Institute and State University, Blacksburg, Virginia

Noah H. Schiller and Travis L. Turner
Langley Research Center, Hampton, Virginia

September 2013

NASA STI Program . . . in Profile

Since its founding, NASA has been dedicated to the advancement of aeronautics and space science. The NASA scientific and technical information (STI) program plays a key part in helping NASA maintain this important role.

The NASA STI program operates under the auspices of the Agency Chief Information Officer. It collects, organizes, provides for archiving, and disseminates NASA's STI. The NASA STI program provides access to the NASA Aeronautics and Space Database and its public interface, the NASA Technical Report Server, thus providing one of the largest collections of aeronautical and space science STI in the world. Results are published in both non-NASA channels and by NASA in the NASA STI Report Series, which includes the following report types:

- TECHNICAL PUBLICATION. Reports of completed research or a major significant phase of research that present the results of NASA Programs and include extensive data or theoretical analysis. Includes compilations of significant scientific and technical data and information deemed to be of continuing reference value. NASA counterpart of peer-reviewed formal professional papers, but having less stringent limitations on manuscript length and extent of graphic presentations.

- TECHNICAL MEMORANDUM. Scientific and technical findings that are preliminary or of specialized interest, e.g., quick release reports, working papers, and bibliographies that contain minimal annotation. Does not contain extensive analysis.

- CONTRACTOR REPORT. Scientific and technical findings by NASA-sponsored contractors and grantees.

- CONFERENCE PUBLICATION. Collected papers from scientific and technical conferences, symposia, seminars, or other meetings sponsored or co-sponsored by NASA.

- SPECIAL PUBLICATION. Scientific, technical, or historical information from NASA programs, projects, and missions, often concerned with subjects having substantial public interest.

- TECHNICAL TRANSLATION. English-language translations of foreign scientific and technical material pertinent to NASA's mission.

Specialized services also include organizing and publishing research results, distributing specialized research announcements and feeds, providing information desk and personal search support, and enabling data exchange services.

For more information about the NASA STI program, see the following:

- Access the NASA STI program home page at *http://www.sti.nasa.gov*

- E-mail your question to help@sti.nasa.gov

- Fax your question to the NASA STI Information Desk at 443-757-5803

- Phone the NASA STI Information Desk at 443-757-5802

- Write to:
  STI Information Desk
  NASA Center for AeroSpace Information
  7115 Standard Drive
  Hanover, MD 21076-1320

NASA/TM–2013-218041

Active Noise Control of Radiated Noise From Jets

Michael J. Doty
Langley Research Center, Hampton, Virginia

Christopher R. Fuller
Virginia Polytechnic Institute and State University, Blacksburg, Virginia

Noah H. Schiller and Travis L. Turner
Langley Research Center, Hampton, Virginia

National Aeronautics and
Space Administration

Langley Research Center
Hampton, Virginia 23681-2199

September 2013

Acknowledgments

The authors sincerely thank graduate students Susana Acosta and Adam Slagle for their assistance in this research. In addition, the efforts of the Jet Noise Lab technical staff (Harry Haskin, John Swartzbaugh, Shaun Reno, James Allen, and Mike Carr) are gratefully acknowledged. Lastly, 3-D printing of various nozzle configurations by Suzanne Zaremski of the National Institute of Aerospace is much appreciated.

Available from:

NASA Center for AeroSpace Information
7115 Standard Drive
Hanover, MD 21076-1320
443-757-5802

Abstract

The reduction of jet noise using a closed-loop active noise control system with high-bandwidth active chevrons was investigated. The high frequency energy introduced by piezoelectrically-driven chevrons was demonstrated to achieve a broadband reduction of jet noise, presumably due to the suppression of large-scale turbulence. For a nozzle with one active chevron, benefits of up to 0.8 dB overall sound pressure level (OASPL) were observed compared to a static chevron nozzle near the maximum noise emission angle, and benefits of up to 1.9 dB OASPL were observed compared to a baseline nozzle with no chevrons. The closed-loop actuation system was able to effectively reduce noise at select frequencies by 1-3 dB. However, integrated OASPL did not indicate further reduction beyond the open-loop benefits, most likely due to the preliminary controller design, which was focused on narrowband performance.

I. Introduction

This report describes results from Phase I of an Aeronautics Research Mission Directorate (ARMD) Seedling Fund project recently investigated at NASA Langley Research Center. The overall goal of this work is to reduce jet noise using a closed-loop active noise control system with high-bandwidth active chevrons.

Aircraft noise is considered to be the most significant barrier to increasing the capacity of the national airspace system. The scope of the problem is underscored by the fact that the FAA has spent $5B on airport noise abatement programs since 1980[1]. Jet noise is considered to be a dominant source of aircraft noise, particularly at takeoff. Therefore, jet noise can adversely affect communities near airports, airline passengers, and military personnel supporting aircraft operations. For instance, Veterans Affairs now spends over $100 million a year in hearing loss benefits to veterans often exposed to high jet noise levels[2].

While techniques to reduce jet noise have been studied for several decades, one recent advancement is the evolution of chevrons (serrations) at the nozzle trailing edge. Chevrons introduce streamwise vorticity into the jet shear layer, increasing mixing and decreasing the jet potential core length. In turn, the low frequency jet noise associated with large-scale turbulence is typically reduced, while high frequency jet noise due to smaller-scale turbulence near the nozzle exit is often increased. Balancing the low frequency noise benefit with the high frequency noise penalty to get a net beneficial noise reduction is essential to a good chevron design. Furthermore, while chevrons can impact jet thrust, slight modifications to the nozzle exit area can minimize thrust penalties.

This work examines the use of vibrating chevrons to enhance the noise reduction potential of passive chevrons with a high-frequency, active excitation. Previous researchers have shown that small-scale, high-frequency perturbations near the nozzle exit can be used to modify the initial growth rate of the mixing layer[3] and thereby reduce jet noise[4]. Introducing additional high-frequency energy at the nozzle exit is believed to increase the production of small-scale disturbances at the expense of large-scale turbulence. These large-scale turbulent structures are responsible for the dominant portion of the jet mixing noise occurring in subsonic transports and military jets at takeoff. Additionally, these turbulent structures play an important role in broadband shock-associated noise generation in off-design supersonic jet flows typical of subsonic transports operating at cruise altitude or military jets at takeoff. Therefore, by exciting the typically static chevron geometry at high frequency, an additional acoustic benefit is

anticipated. This approach requires minimal power and differs from existing active jet noise control techniques such as plasma actuation and fluidic injection, which require substantial power and mass flow requirements, respectively.

Furthermore, recent numerical simulations suggest that relatively small perturbations at the nozzle lip may be sufficient to reduce jet noise by 6-9 dB[5,6]. However, this level of reduction requires optimal time-accurate perturbations, which cannot be achieved using open-loop configurations. Consequently, the current effort employs an adaptive closed-loop control configuration in which the adaptive algorithm adjusts the drive signals to the chevrons to minimize the far-field radiated sound in real time. A feedforward control strategy was implemented as shown in Fig. 1 using the filtered-reference least mean squares (FXLMS) algorithm. A near-field microphone was used as a reference sensor for the adaptive feedforward controller. The output of the controller was used to drive the high-bandwidth active chevron with oscillating signals. Although the feedforward approach is most effective when the reference sensor is able to provide information prior to the control, such an arrangement is not possible in this application. Therefore, for proof-of-concept investigations, a bandpass filter was applied to the broadband signal, typically at the resonant frequency of the nozzle system.

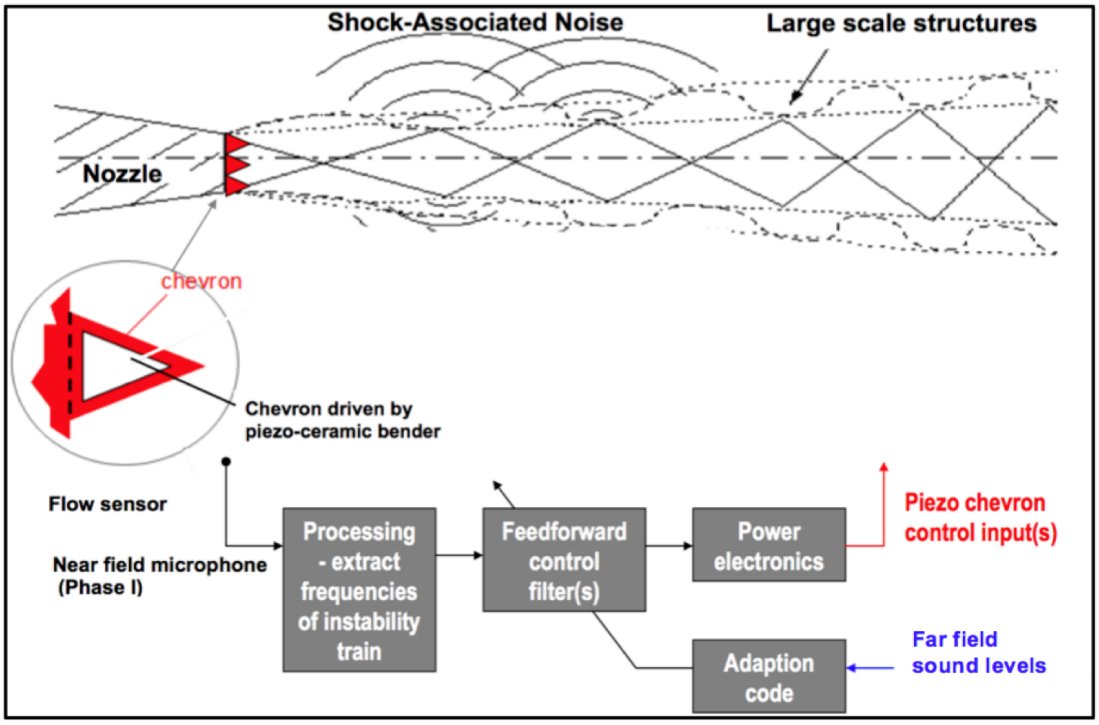

Figure 1. Schematic of feedforward active noise control system.

The objective of this work is to demonstrate the potential of closed-loop active noise control with high-bandwidth active chevrons to reduce jet noise. The next section of the report describes the facility, nozzles, and excitation hardware as well as the instrumentation, and data acquisition/processing in greater detail. Section III examines the experimental results including chevron tip penetration studies and the open-loop and closed-loop excitation acoustic results. Finally, Section IV ends the report with concluding remarks and a discussion of future work.

II. Experimental Procedures

A. Facility

All jet noise experiments took place in the Small Anechoic Jet Facility (SAJF) at NASA Langley Research Center. The facility shown in Fig. 2 consists of a single stream jet flow capable of delivering up to 2 lbm/s of air. A Chromalox heater of 275 W is used to raise the stagnation temperature of the jet stream, in this case up to 100° F for consistency throughout the experiments. A 2 ft diameter duct concentric to the nozzle provides a minimal co-flow velocity around the jet flow when operating a single speed fan in the exhaust duct; however, it was not used in the current work. The jet exhausts into an anechoic chamber. The chamber contains fiberglass wedges and tip-to-tip dimensions of 12.7 ft long x 8.4 ft wide x 10.7 ft high providing an anechoic environment down to 250 Hz.

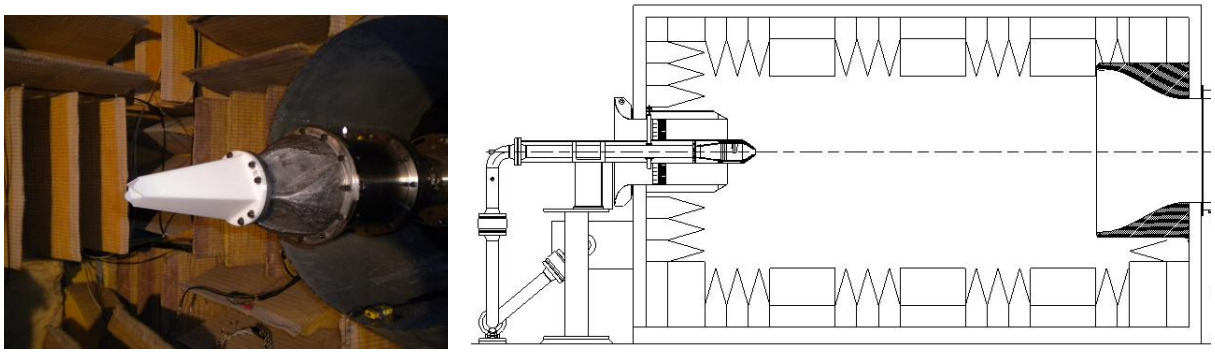

a) **b)**

Figure 2. Small Anechoic Jet Facility (SAJF) a) with installed chevron nozzle and b) facility schematic.

B. Nozzles

To simplify the chevron actuation process, flat-sided rectangular nozzles were fabricated for this study. A converging-diverging contoured nozzle was designed using the Method of Characteristics for a design Mach number of M=1.5 as shown in Fig. 3a. In the diverging section of the nozzle one pair of opposite walls remained parallel while the other pair diverged. The nozzle throat is 1 inch square while the nozzle exit is slightly larger, as shown in Fig. 3b, resulting in an equivalent diameter at the nozzle exit of D_{eq}=1.224".

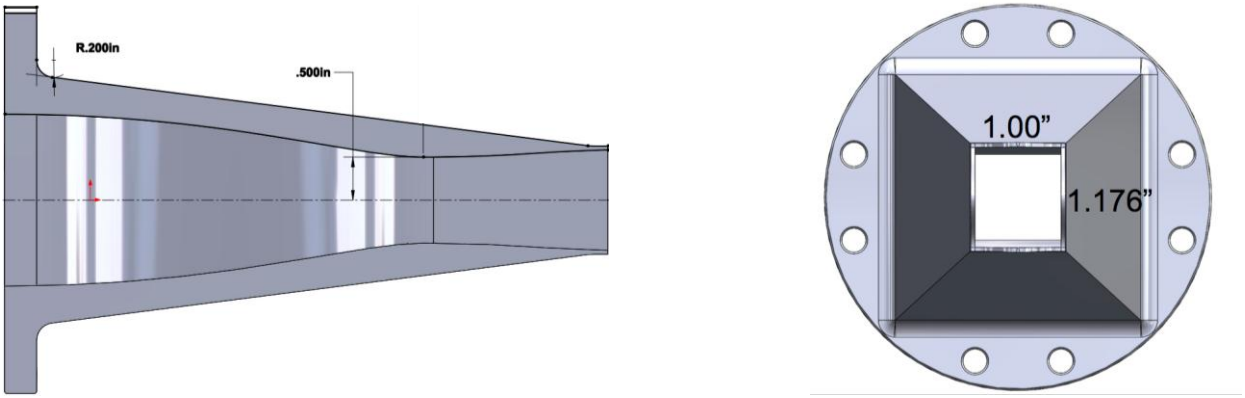

a) **b)**

Figure 3. Nozzle geometry including a) contour and b) exit plane.

Chevron designs were scaled from previous work with Boeing[7] with the chevron width extending to the full sidewall dimension and chevron length equal to 0.390". The initial chevron nozzle design in which the chevrons followed the diverging nozzle contour (Fig. 4a) was not effective. Therefore, converging chevrons with various levels of penetration into the jet plume were considered (Fig. 4b). Penetration depths, defined as the distance from the projected diverging nozzle contour to the chevron tip, of 0.050", 0.100", and 0.150" were considered. Section IIIB describes the results of these chevron penetration investigations. The nozzles were all fabricated from ABS plastic using a 3-D printer. This manufacturing proved cost effective and efficient; however, some cracking near the chevron root was observed when running at supersonic Mach numbers. This problem was mitigated by reinforcing the chevron roots of the non-excited chevrons with metal plates as shown in Fig. 5.

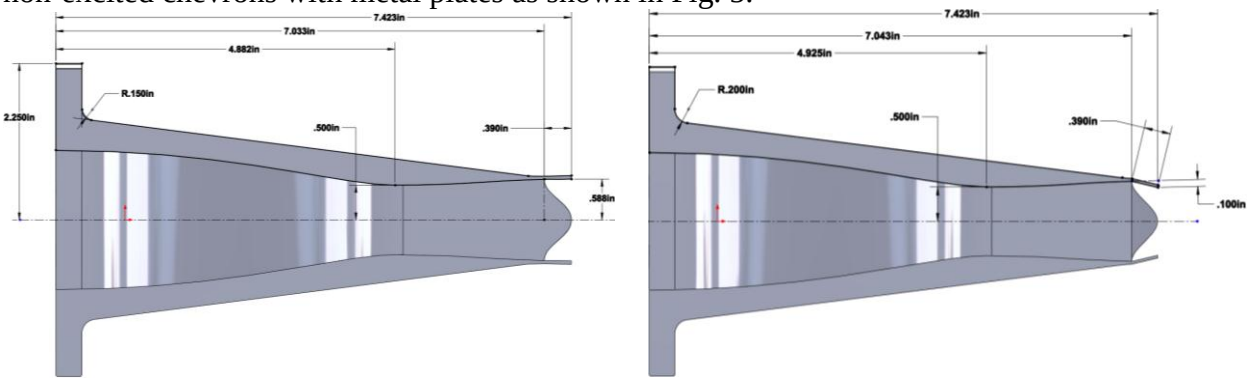

a) **b)**

Figure 4. Chevron nozzle with chevrons a) following diverging contour and b) converging.

Figure 5. Chevron nozzle reinforced with metal plates and tape.

C. Excitation Hardware

Several chevron excitation schemes were considered, and two were downselected for initial testing as shown in Fig. 6. Figure 6a shows a Macro Fiber Composite (MFC) piezoelectric patch actuator that was bonded to the outside of the chevron with strain gauge adhesive. A mechanical shaker with a sting attached to a clevis and nylon hinge arrangement is shown in Fig. 6b. Although the mechanical shaker provided more significant displacement authority than the MFC, the shaker arrangement would not effectively operate at frequencies above 100 Hz. Therefore, the superior frequency response and robustness of the MFC led to its downselection as the primary excitation method. For simplicity, this initial work focused on the excitation of a single chevron, unless otherwise noted. Interestingly, the stiffness of the MFC actuator was sufficient to avoid the chevron cracking issue previously discussed so no further reinforcement was necessary for the excited chevron.

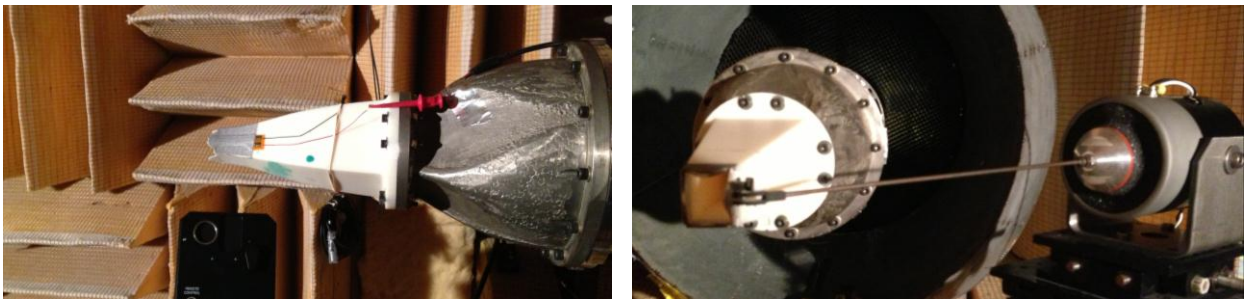

a) **b)**

Figure 6. a) MFC piezoelectric patch actuator and b) mechanical shaker and sting with clevis/hinge attachment.

D. Instrumentation

1. Tip Displacement Measurements

The determination of the chevron tip displacement during actuation was accomplished in one of several ways. An accelerometer was often placed directly on the chevron for initial characterization. However, to avoid the effects of the added mass of the accelerometer on the system during testing, a laser vibrometer was used for tip displacement measurements. When inconsistencies with the vibrometer were discovered at very low excitation frequencies, the vibrometer was replaced with a Keyence laser displacement sensor shown in Fig. 7 as the primary instrument for determining tip displacement.

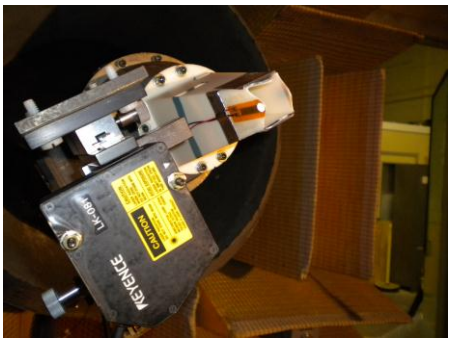

Figure 7. Laser displacement sensor mounted on opposite side of nozzle from far-field microphones.

2. Acoustic Measurements

Far-field acoustic measurements were made with a linear array of seven Brüel and Kjær (B&K) Model 4939 free-field microphones of 0.25 inch diameter in conjunction with Model 2670 pre-amplifiers and a B&K Multiplexer (Model 2811). The polar range of the microphones was from 75° to 150° from the upstream jet axis, and the microphones were located on an azimuthal plane nominally 30° above the jet centerline pointed toward the jet exit. The nozzles were also mounted with a 30° clocking so that the microphone plane intersected the chevron tips on each side of the nozzle. Electrostatic and pistonphone calibrations were routinely performed on all microphones, and the grid caps were removed for testing. Two additional 0.25 inch microphones were also employed as reference and error sensors, respectively, for the closed-loop control implementation that will be further discussed in Section IIID.

E. Data Acquisition and Processing

The SAJF data acquisition system consists of a series of LabVIEW virtual instruments running on an acquisition PC. The eight channels of dynamic signals (seven microphone and one tip displacement) are routed through high pass (100 Hz) and low pass (102,300 Hz) Precision filters with autogaining applied to the signals. A National Instruments PCI-6143 8 channel simultaneous sampling multi-function data acquisition board receives the signals. The dynamic signal data are acquired at 210 kHz with 180 data averages, resulting in a 4096-point spectrum with a frequency resolution of 25.63 Hz. Microphone frequency response and free-field response corrections were applied, and atmospheric attenuation corrections to a lossless condition were applied according to the ANSI standard[8]. The corrected far-field spectral levels were then propagated to a common distance of 100 jet diameters from the nozzle exit. These corrections have been applied to all far-field microphone data unless otherwise noted.

An example of the repeatability of the far-field microphone array is shown in Fig. 8 for M=0.9 at the sideline angle (90°) and near maximum noise emission angle (150°) from the jet inlet axis. Comparisons in this report have typically been made only for data taken during the same day to minimize day-to-day uncertainty. Nonetheless, Fig. 8 shows consistency between data taken on different days within 0.12 OASPL. Similar levels of repeatability were also common at supersonic conditions.

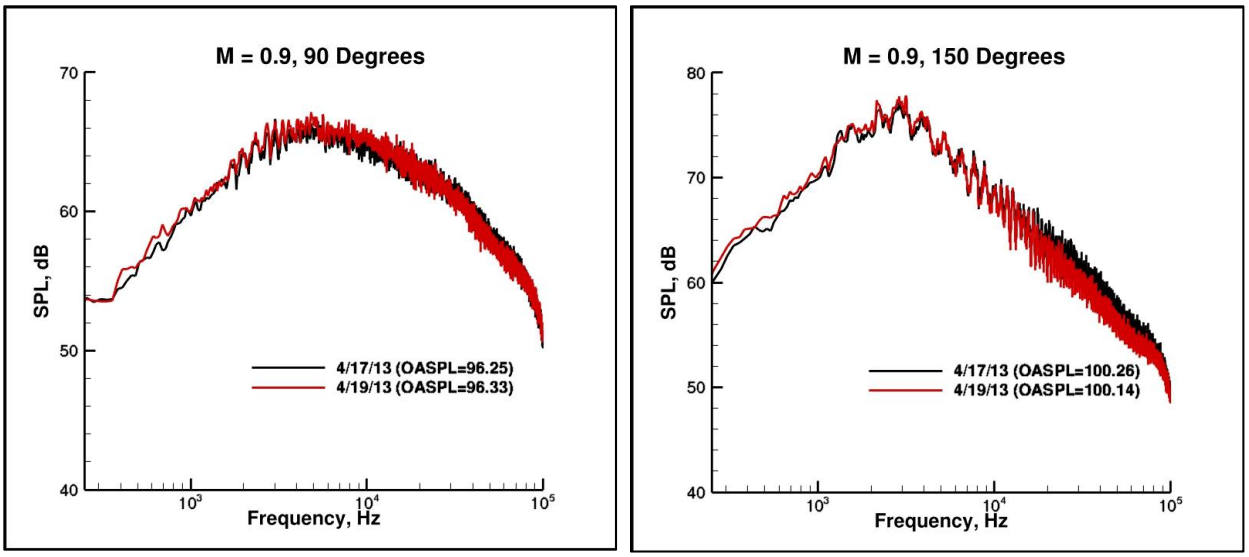

a) **b)**

Figure 8. Far-field acoustic results at M=0.9 showing repeatability at a) 90° and b) 150° from the jet inlet axis.

III. Experimental Results

A. Flow Conditions

The flow conditions examined in this work are shown in Table 1 including Mach number, M, and characteristic frequency, f_c. The results focus on conditions representative of subsonic commercial takeoff (M=0.9) and supersonic, over-expanded conditions typical of military takeoff (M=1.4) as highlighted in Table 1.

Table 1. Typical experimental conditions assuming standard day conditions.

NPR	*M*	T_T (°R)	$f_c = U_j/D_j$ (Hz)
1.064	0.3	560	3,370
1.692	0.9	560	9,497
2.77	1.3	560	12,778
3.182	1.4	560	13,493
3.67	1.5	560	14,164
4.25	1.6	560	14,796

B. Tip Penetration Studies

Before proceeding with actuation of the chevrons, an investigation of static chevron tip penetration was undertaken. A baseline nozzle (no chevrons) was compared to three increasing chevron penetrations (0.050", 0.100", and eventually 0.150"). Figure 9 shows the *M*=0.9 far-field acoustic spectral results at the sideline angle (90°) and near maximum noise emission angle (150°) from the jet inlet axis. The low frequency benefit and high frequency penalty commonly seen with increasing chevron penetration is generally observed. Integrated OASPL tend to increase with increasing chevron penetration at 90° and decrease with increasing chevron penetration at 150°, indicative of the relative importance of high and low frequency noise at each angle. Although the 0.100" penetration case was further investigated in the current effort due to timing and availability of additional nozzle hardware, the 0.150" penetration case also shows promise acoustically and will be further investigated. The high frequency noise of the 0.150" penetration case is lower than, or on par with, the 0.100" nozzle results while showing noticeably more low frequency benefit. The decrease in high frequency penalty going from the 0.100" to the 0.150" penetration case may be due to the difference in corner flow associated with different chevron penetrations for these rectangular nozzles. These results also highlight the importance of displacement for the control effect of the vibrating active chevron.

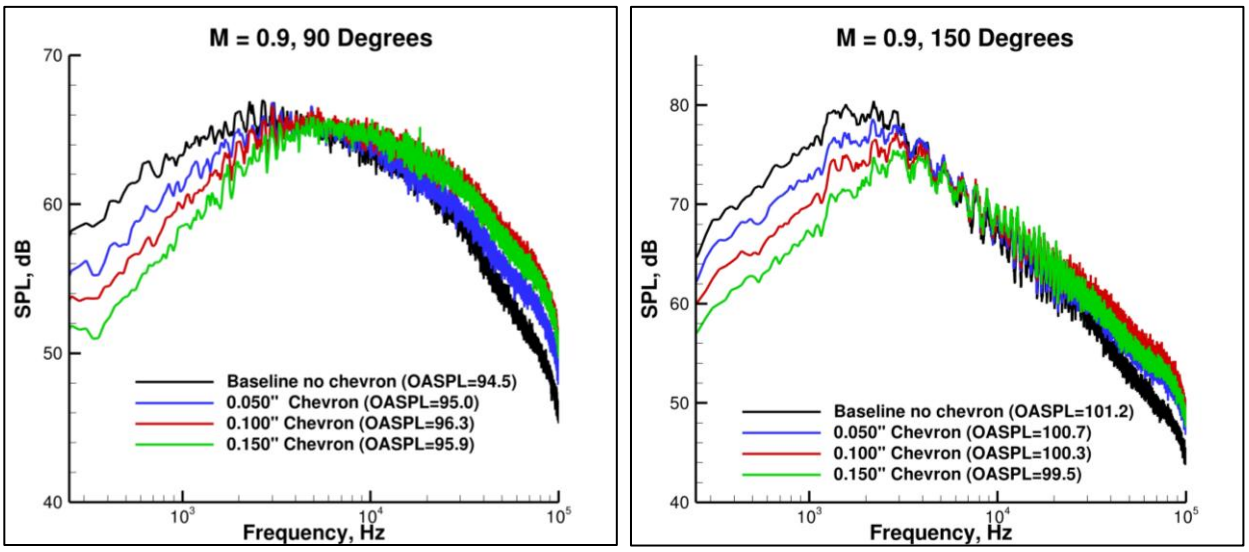

a) **b)**

Figure 9. Far-field acoustic results at *M*=0.9 for several chevron penetrations at a) 90° and b) 150° from the jet inlet axis.

C. Open-Loop Excitation Results

Prior to acoustic testing, an MFC piezoelectric patch actuator was placed on a single chevron, covered with reflective tape, and measured using a laser vibrometer as shown in Fig. 10. The nozzle resonant frequency was typically found to be near 1000 Hz, with the value changing slightly once installed in SAJF. The chevron was then excited at the nozzle resonant frequency to maximize displacement. As seen in Fig. 10, the maximum tip displacement due to excitation is approximately 0.1 mm (0.004").

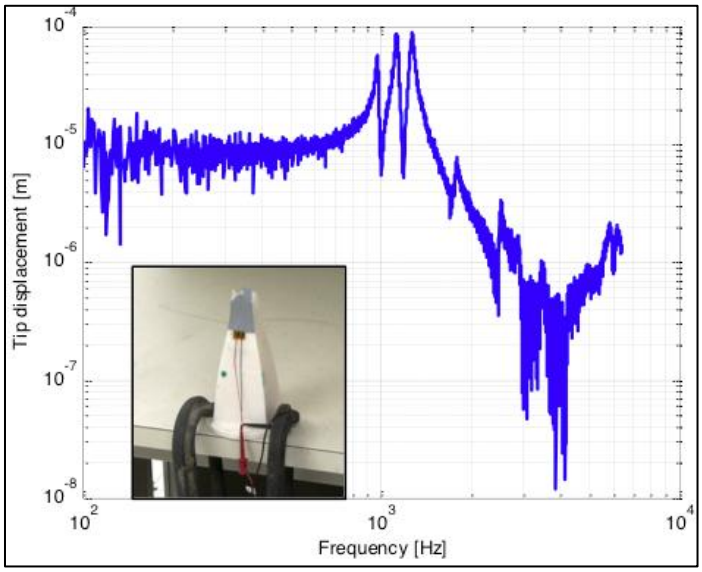

Figure 10. Benchtop tip displacement measurements of excited chevron.

The characterized system was then assembled in the SAJF, and the chevron with the MFC was located in the azimuthal location closest to the far-field microphone array. Figure 11 shows the open-loop excitation results for the 0.100" penetration chevron nozzle at the resonant frequency of the nozzle. The excitation results are compared to both the static chevron (no excitation) case and the baseline no chevron case at M=0.9 and M=1.4.

For the M=0.9 case of Fig. 11a at 90°, the excited chevron shows a slight spectral reduction across a broad frequency range compared to the static chevron. At the excitation frequency of 1020 Hz, the exited chevron spectrum shows a narrowband peak several dB above the static chevron spectrum. From an integrated OASPL perspective, the excited chevron reduces the penalty (noise increase associated with static chevrons at this angle) of the static chevron by 0.4 dB OASPL. For the 150° case of Fig. 11b the excited chevron shows a similar benefit across the spectrum. Furthermore, the excited chevron increases the static chevron benefit by 0.8 dB OASPL. Considering only one of the four chevrons is excited in these cases, and at displacements of a few thousandths of an inch, the potential for more significant noise reduction with additional excited chevrons and greater excitation displacements is anticipated.

The slightly overexpanded supersonic condition of M=1.4 is shown in Figs. 11c and 11d. The excitation frequency has increased slightly to 1050 Hz to match the changing resonant frequency of the system at this flow speed. In Fig. 11c at 90°, the dominance of broadband shock-associated noise above 10 kHz is noted. Furthermore, the increase in broadband-associated shock noise with the addition of chevrons, also observed in other work[9], is evident here. The chevron excitation does not noticeably alter the broadband shock-associated noise, perhaps

because more significant chevron tip displacements are required. At a further downstream angle where shock noise is no longer dominant, as shown in Fig. 11d, the excited chevron shows additional benefit beyond the static chevron of 0.3 dB OASPL. Thus, the excited chevron case again shows benefits beyond the static chevron case for reducing jet mixing noise.

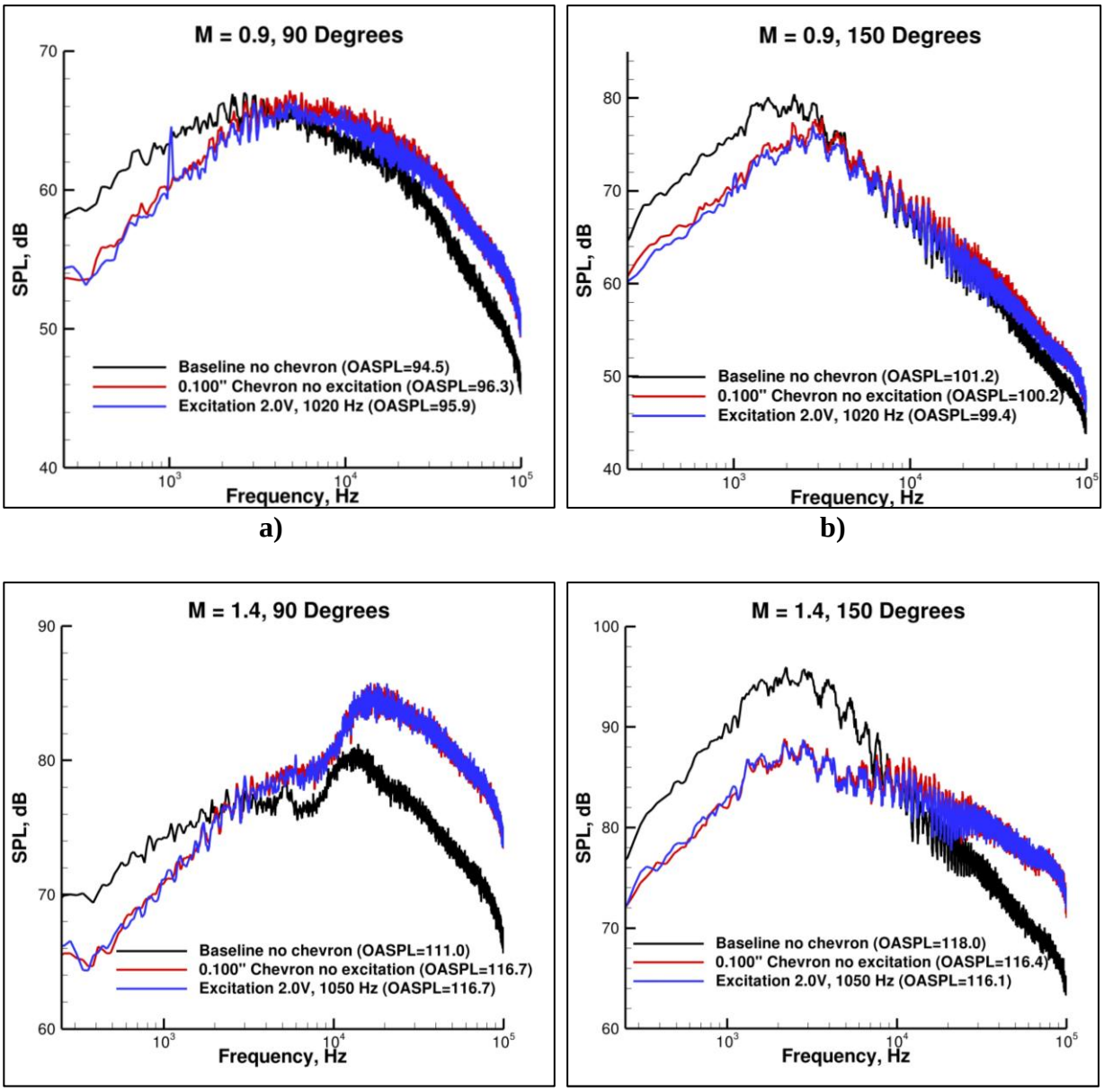

Figure 11. Open-loop far-field acoustic results with open-loop excitation at the nozzle resonant frequency for *M*=0.9 at a) 90° and b) 150° and for an overexpanded supersonic case at *M*=1.4 at c) 90° and d) 150°.

D. Closed-Loop Excitation Results

Implementation of the closed-loop control strategy involved the use of a digital feedforward control approach utilizing the filtered-reference least mean squares (FXLMS) algorithm with feedback cancellation in the time domain. A block diagram of the FXLMS approach is shown in Fig. 12a. The feedforward approach requires a reference signal that is highly correlated with the noise to be cancelled. That signal is then fed forward through an adaptive Finite Impulse Response (FIR) filter, and the filter output is used to drive a control source. The adaptive filter is adjusted in real time by monitoring the radiated field with an error sensor and utilizing the LMS algorithm to adapt the FIR filter coefficients.

The active controller was first tested in a benchtop experiment using broadband sound waves generated in a long tube utilizing a speaker at one end driven by white noise. The drive signal to the noise source was also used as the reference signal to the controller. An active sound speaker was located near the duct outlet and driven by the output of the controller. A microphone was located in the radiated sound field and was used as an error sensor for the controller. In practice, the use of a far-field microphone may not be feasible on aerospace vehicles. Thus, the development of a virtual sensor, as previously demonstrated by Papenfuss *et al.*[10], may ultimately be required.

The noise source was turned on, and the spectrum of the uncontrolled sound level was measured from the error sensor output. The controller was then turned on and allowed to converge, and then the spectrum at the error sensor was re-measured. The results are shown in Fig. 12b, demonstrating the controller provides significant reduction of the sound across a broad frequency range.

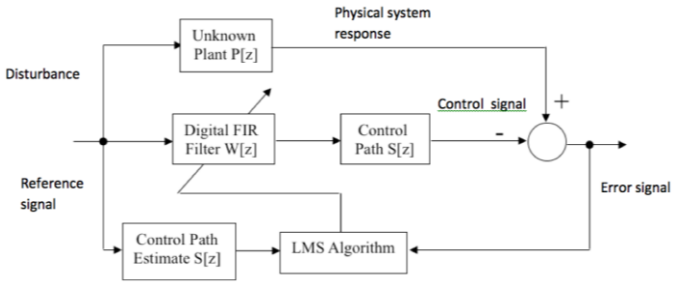

a)

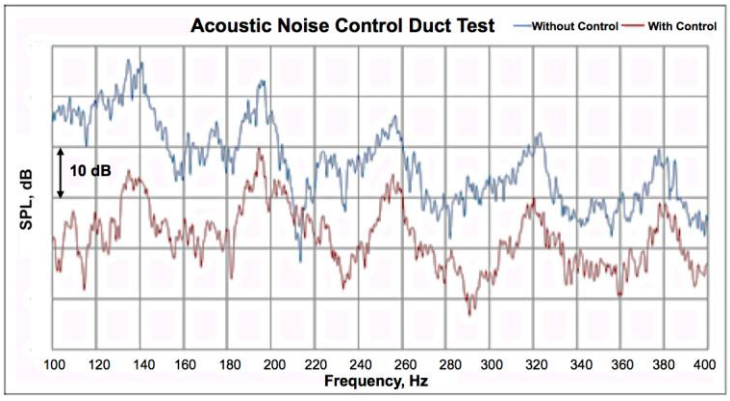

b)

Figure 12. a) Block diagram of feedforward arrangement and b) example benchtop performance of active noise control system.

Following the benchtop demonstration of the closed-loop feedforward control strategy, the system was implemented in the SAJF. The reference sensor was a near/mid field microphone, and an additional far-field microphone at approximately 155° was utilized as the error sensor. The output of the adaptive filter was used to drive the piezoelectric actuator on the chevron. This control strategy is most effective when the reference sensor provides time-advanced information correlated with the disturbance, which was not possible in this configuration. Therefore, a band-pass filter was used to filter the broadband signal from the near/mid field microphone to generate a narrowband reference signal. This reduced the need for a time-advanced reference; however, it also limited the bandwidth of the controller. Figure 13 shows the noise reduction for the closed-loop control strategy at the far-field error sensor microphone at the targeted frequency, which was typically the excitation frequency of the system. In this case two chevrons were excited out of phase, but the results were similar for various excitation arrangements in that the closed-loop control system routinely decreased noise at a single frequency by 1-3 dB.

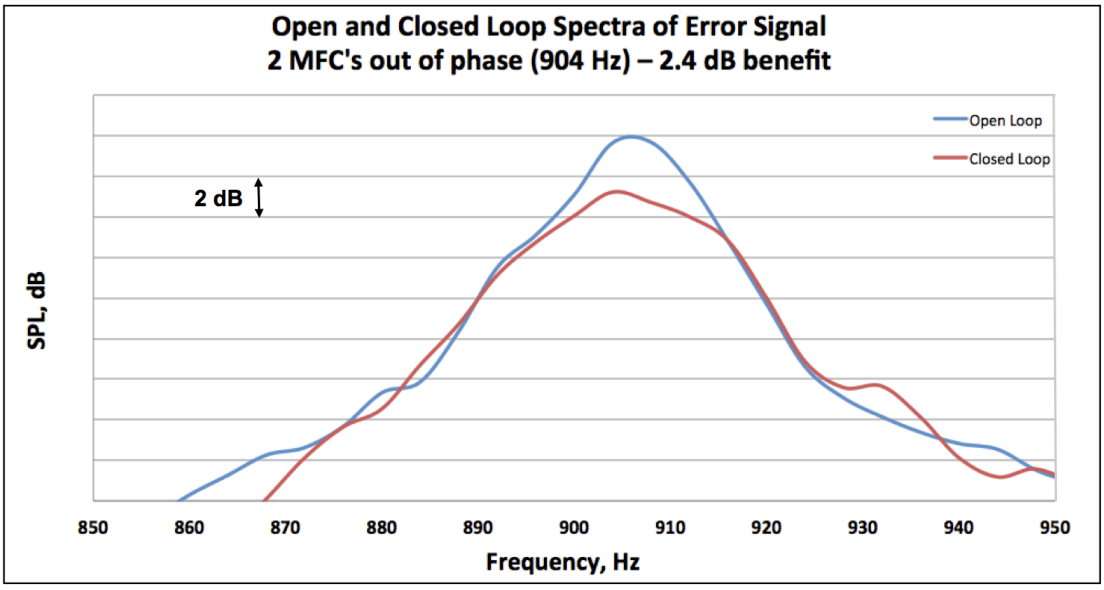

Figure 13. Reduction of uncorrected jet noise spectrum near 900 Hz due to control system.

Nonetheless, because the reference signal was bandpass filtered, the benefit of the closed-loop control on the overall sound pressure level of broadband jet noise was not as significant as the single frequency benefit. Figure 14 shows that with two chevrons excited in phase at 1800 Hz, there is a high frequency increase of 0.7 OASPL at 90° (Fig. 14a) compared to the unexcited chevron case. On the other hand, active control reduces the noise at 150° (Fig. 14b) by 0.6 dB OASPL compared to the unexcited chevron case. This level of benefit is similar to the open-loop result of Fig. 11b. There are several portions of the low-to-mid frequency spectra in Fig. 14 that are reduced by 2-3 dB with closed-loop actuation. The attenuation is likely to be improved with an increased number of active chevrons and an adjustment of the control paradigm, both planned in future project work.

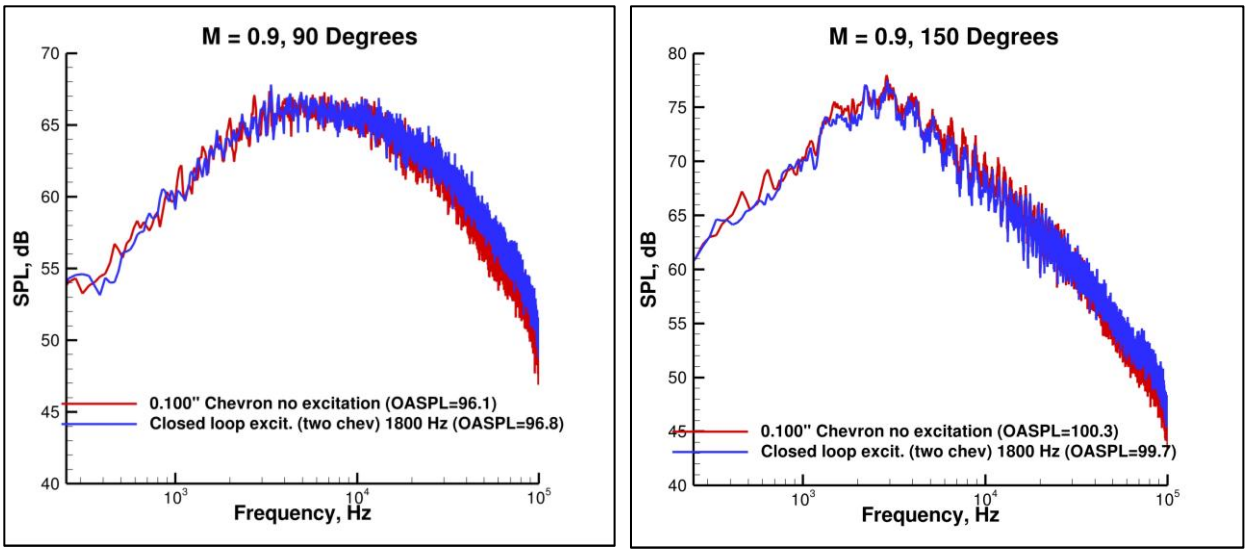

a) **b)**

Figure 14. Closed-loop far-field acoustic results at *M*=0.9 at a) 90° and b) 150°.

IV. Concluding Remarks

A closed-loop active noise control system using high-bandwidth active chevrons was demonstrated in a proof-of-concept work. The active chevron system has shown promise in reducing far-field noise levels beyond what static chevrons can achieve.

To accomplish this work, a piezoelectric patch actuator was downselected as the primary actuation scheme and integrated with an ABS plastic supersonic rectangular jet nozzle. Benchtop experiments characterized the actuation frequency and tip displacement of the chevron. Concurrently, an acoustic investigation of various static chevron tip penetration depths was conducted, leading to the downselection of a 0.100" static chevron tip displacement nozzle. The active chevron nozzle system was installed in the SAJF, and the open-loop performance was assessed at various jet Mach numbers while exciting a single chevron. Benefits of up to 0.8 dB OASPL were observed compared to a static chevron nozzle near the maximum noise emission angle, and benefits of up to 1.9 dB OASPL were observed compared to a baseline nozzle with no chevrons. The excited chevron did not reduce the broadband shock-associated noise – more significant chevron tip displacements would likely be required for that. In parallel efforts, a digital feedforward control algorithm was shown to reduce noise in a benchtop test using a speaker tube. The closed-loop actuation system was installed in the SAJF and results showed that the adaptive system was able to effectively reduce noise at select frequencies by 1-3 dB. However, integrated OASPL did not show any significant further reduction beyond the open-loop benefits, most likely due to the controller being designed for narrowband performance.

Future work will focus on increasing both the number of active chevrons around the periphery of the nozzle as well as the chevron tip displacement. Pre-stressed piezo-ceramic actuators show an order of magnitude increase in displacement authority over conventional MFC actuators. Stainless steel substrates are being custom-designed to incorporate excitation of the entire chevron geometry. In addition, the expansion of the control strategy beyond select frequencies is planned using various feedback control approaches. Finally, increasing the understanding of the effects of the actuation on the flowfield by incorporating Particle Image Velocimetry (PIV)

measurements and moving to faceted axisymmetric nozzles of larger scale are additional planned investigations.

References

[1] Strazisar, T., "Aeronautics Research at NASA," presented at the Fundamental Aeronautics 2011 Annual Meeting, March 15, 2011.

[2] Doychak, J., "Department of Navy Jet Noise Reduction Project Overview," presented at the 15th Annual Partners in Environmental Technology Technical Symposium and Workshop, December 1, 2010.

[3] Parekh, D., Kibens, V., Glezer, A., Wiltse, J., and Smith, D., "Innovative Jet Flow Control – Mixing Enhancement Experiments," AIAA Paper 96-0308, presented at the 34th AIAA Aerospace Sciences Meeting, January 1996.

[4] Butler, G. and Calkins, F., "Initial Attempts to Suppress Jet Noise Using Piezoelectric Actuators," AIAA Paper 2003-3192, presented at the 9th AIAA/CEAS Aeroacoustics Conference, May 2003.

[5] Babucke, A., Spagnoli, B., Airiau, C., Kloker, M., and Rist, U., "Mechanisms and Active Control of Jet-Induced Noise," *Numerical Simulation of Turbulent Flows and Noise Generation*, NNFM Vol. 104, Springer Verlag, 2009.

[6] Freund, J., "Adjoint-based Optimization for Understanding and Suppressing Jet Noise," IUTAM Symposium on Computational Aero-Acoustics for Aircraft Noise Prediction, Procedia Engineering 6, 2010.

[7] Thomas, R., Czech, M. and Doty, M., "High Bypass Ratio Jet Noise Reduction and Installation Effects Including Shielding Effectiveness," AIAA Paper 2013-0541, presented at the 51st AIAA Aerospace Sciences Meeting, January 2013.

[8] "Method for the Calculation of the Absorption of Sound by the Atmosphere," ANSI S1.26-1978, (ASA 23-1978), American Nat. Stand. Inst., Inc., June 23, 1978.

[9] Henderson, B. and Bridges, J., "An MDOE Investigation of Chevrons for Supersonic Jet Noise Reduction," AIAA Paper 2010-3926, presented at the 16th AIAA/CEAS Aeroacoustics Conference, June 2010.

[10] Papenfuss, C., Saux, T., and Fuller, C., "Design and Implementation of Passive and Multi-Channel Active Noise Treatment of a 2 kW Diesel Generator," Proceedings of the 83rd Shock and Vibration Conference, Williamsburg, VA, June 2012.

REPORT DOCUMENTATION PAGE

Form Approved
OMB No. 0704-0188

1. REPORT DATE *(DD-MM-YYYY)*	2. REPORT TYPE	3. DATES COVERED *(From - To)*
01- 09 - 2013	Technical Memorandum	

4. TITLE AND SUBTITLE

Active Noise Control of Radiated Noise From Jets

5a. CONTRACT NUMBER

5b. GRANT NUMBER

5c. PROGRAM ELEMENT NUMBER

6. AUTHOR(S)

Doty, Michael J.; Fuller, Christopher R.; Schiller, Noah H.; Turner, Travis L.

5d. PROJECT NUMBER

5e. TASK NUMBER

5f. WORK UNIT NUMBER

694478.02.93.02.12.37.23

7. PERFORMING ORGANIZATION NAME(S) AND ADDRESS(ES)

NASA Langley Research Center
Hampton, VA 23681-2199

8. PERFORMING ORGANIZATION REPORT NUMBER

L-20325

9. SPONSORING/MONITORING AGENCY NAME(S) AND ADDRESS(ES)

National Aeronautics and Space Administration
Washington, DC 20546-0001

10. SPONSOR/MONITOR'S ACRONYM(S)

NASA

11. SPONSOR/MONITOR'S REPORT NUMBER(S)

NASA/TM-2013-218041

12. DISTRIBUTION/AVAILABILITY STATEMENT

Unclassified - Unlimited
Subject Category 71
Availability: NASA CASI (443) 757-5802

13. SUPPLEMENTARY NOTES

14. ABSTRACT

The reduction of jet noise using a closed-loop active noise control system with high-bandwidth active chevrons was investigated. The high frequency energy introduced by piezoelectrically-driven chevrons was demonstrated to achieve a broadband reduction of jet noise, presumably due to the suppression of large-scale turbulence. For a nozzle with one active chevron, benefits of up to 0.8 dB overall sound pressure level (OASPL) were observed compared to a static chevron nozzle near the maximum noise emission angle, and benefits of up to 1.9 dB OASPL were observed compared to a baseline nozzle with no chevrons. The closed-loop actuation system was able to effectively reduce noise at select frequencies by 1-3 dB. However, integrated OASPL did not indicate further reduction beyond the open-loop benefits, most likely due to the preliminary controller design, which was focused on narrowband performance.

15. SUBJECT TERMS

Active control; Aeroacoustics; Chevrons; Jet noise

16. SECURITY CLASSIFICATION OF:			17. LIMITATION OF ABSTRACT	18. NUMBER OF PAGES	19a. NAME OF RESPONSIBLE PERSON
a. REPORT	b. ABSTRACT	c. THIS PAGE			STI Help Desk (email: help@sti.nasa.gov)
					19b. TELEPHONE NUMBER *(Include area code)*
U	U	U	UU	18	(443) 757-5802